Journal of Molecular Spectroscopy **194,** 197–202 (1999)
Article ID jmsp.1998.7789, available online at http://www.idealibrary.com on IDEAL®

FTIR Emission Spectra, Molecular Constants, and Potential Curve of Ground State GeO

Edward G. Lee, Jenning Y. Seto, Tsuyoshi Hirao, Peter F. Bernath, and Robert J. Le Roy

Guelph–Waterloo Centre for Graduate Work in Chemistry and Biochemistry, University of Waterloo, Waterloo, Ontario N2L 3G1, Canada

Received September 21, 1998; in revised form November 9, 1998

Extensive new high-temperature, high-resolution FTIR emission spectroscopy measurements for the five common isotopomers of GeO are combined with previous diode laser and microwave measurements in combined isotopomer analyses. New Dunham expansion parameters and an accurate analytical potential energy function are determined for the ground $X^1\Sigma^+$ state. © 1999 Academic Press

I. INTRODUCTION

As one of the important oxides of group IVa elements, germanium monoxide (GeO) has been studied extensively, both theoretically (*1–4*) and in a variety of experiments, including microwave spectroscopy (*5, 6*), chemiluminescence studies of low-lying electronic states (*7–9*), photoelectron spectroscopy (*10*), electronic absorption (*11–13*), and emission (*14*) spectroscopy, and in matrix isolation (*15, 16*), and gas-phase infrared spectroscopy (*17*). Summaries of early spectroscopic work were reported by Capelle and Brom (*9*), Huber and Herzberg (*18*), and Żyrnicki (*14*).

The role of GeO in fabricating integrated optics (*19*) and SiGe alloy-based devices (*20*) has sparked a renewed interest in spectroscopic studies of this molecule which would facilitate its use in providing diagnostics. However, the only existing results in the infrared region consist of matrix isolation measurements (*15, 16*), which give approximate vibrational spacings, and a set of accurate gas-phase diode laser measurements involving levels $v = 0-6$ (*17*). While the latter are of very high quality, they consist of only a modest number of lines spanning a limited range of vibrational and rotational energies.

Fourier transform infrared emission spectroscopy is a useful means of studying the vibration–rotation spectra of unstable species such as GeO (*21*). The high sensitivity and continuous coverage of a wide wavenumber range are major factors in making this technique useful (*21*). This paper reports the results of high-temperature FTIR emission spectroscopy studies of the five common isotopomers of the germanium oxide molecule. The results for all five isotopomers are combined with earlier microwave (*5, 6*) and diode laser measurements (*17*) and treated simultaneously in two types of analyses: (i) a conventional Dunham analysis with isotopomer mass scaling which allows for the presence of atomic mass-dependent Born–Oppenheimer breakdown terms, and (ii) a "direct potential fit" analysis which yields an analytic potential energy curve for the system, and again allows for Born–Oppenheimer breakdown terms.

Supplementary data for this article may be found on the journal home page (http://www.academicpress.com/jms).

II. EXPERIMENTAL

The high-resolution infrared emission spectra of GeO were obtained in emission with the experimental setup shown in Fig. 1. The main components of the system are a Bruker IFS-120-HR high-resolution FT spectrometer, a commercial CM Rapid Temp furnace, a 1.2-m long ceramic tube cell with water-cooled end windows, gas lines, a vacuum pump, and pressure-monitoring meters. To obtain the most intense signal possible, appropriate cell windows, beamsplitter, and detector must be chosen for the wavenumber region in question. In the present experiment, a KRS-5 (thallium bromoiodide) end window, a KBr beamsplitter, and a liquid helium-cooled boron-doped Si detector were used.

Five grams of germanium powder (Aldrich) containing the five naturally occurring stable isotopes was placed in the cell. With the cell sealed, overnight pumping was carried out at a temperature of about 200°C to remove impurities (especially water vapor) from the cell. Germanium has a melting point of 934°C. Intensive emission is expected above this temperature, and more ro-vibrational transitions are expected at higher temperatures. With the furnace at its maximum working temperature of 1500°C, 2 Torr of oxygen gas and 18 Torr of argon buffer gas were let into the cell. The valves connected to the cell were kept nearly closed to maintain a high concentration of GeO molecules while minimizing the concentration of interfering species.

To obtain a survey spectrum in a relatively short time (a few minutes), the spectrometer was first set to a resolution of 0.05 cm^{-1}, and 10 scans were co-added. A high-intensity spectrum consisting of clear *P* and *R* branches with sets of evenly spaced

0022-2852/99 $30.00

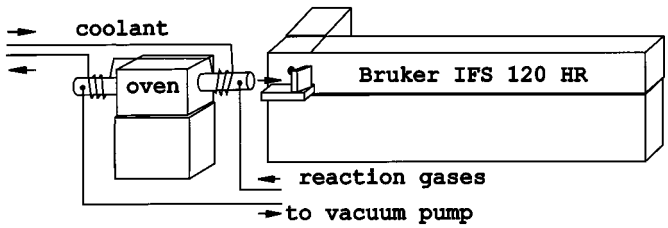

FIG. 1. Schematic diagram of the experimental setup.

lines in the region 800–1100 cm^{-1} appeared and was identified as being due to GeO by comparisons with the line positions obtained in the diode laser experiment of Thompson *et al.* (*17*). A higher resolution spectrum was then recorded by setting the spectrometer resolution to 0.006 cm^{-1} and increasing the number of scans to 30. It took about an hour to complete the recording and the Fourier transform computation. Another spectrum was recorded in the same way and the two were added together to reduce the noise and obtain the final spectrum, which is shown in Fig. 2.

III. RESULTS: MEASUREMENT AND ASSIGNMENT OF SPECTRAL LINES

The five naturally occurring stable isotopes of germanium have relative abundances of 35.9% (^{74}Ge), 27.7% (^{72}Ge), 21.2% (^{70}Ge), 7.7% (^{73}Ge), and 7.4% (^{76}Ge), respectively (*22*). Although there are three naturally occurring oxygen isotopes, ^{16}O is overwhelmingly dominant (99.8% abundance) (*22*) and is the only one observed here. Therefore, only five isotopomers of the GeO species were observed in this work.

The ro–vibrational line positions in the spectrum were measured using J. Brault's computer program PC/DECOMP (*23*). It determines the center of a line by fitting its profile to a Voigt lineshape function, which is a convolution of Gaussian and Lorentzian functions (*24*).

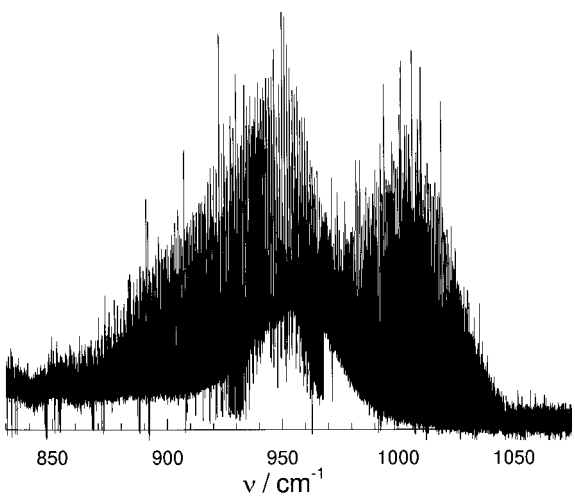

FIG. 2. Overview of the high-temperature FTIR emission spectrum of GeO.

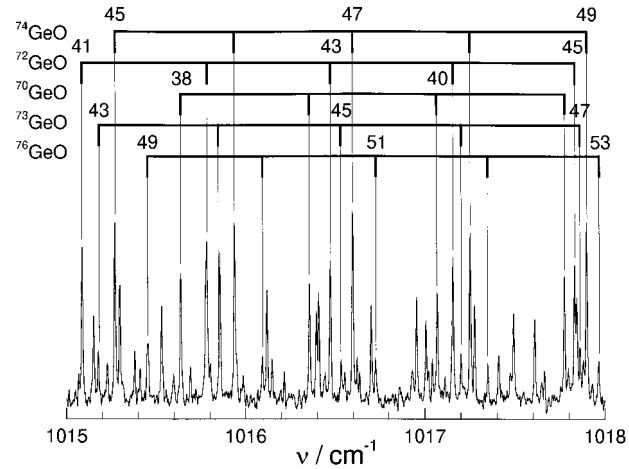

FIG. 3. Segment of the high-temperature FTIR emission spectrum of GeO isotopomers showing assignments for transitions in the *R* branches of their fundamental bands.

A Loomis–Wood program (*25*) and a plot of the spectrum were used to help identify the lines belonging to a given band. The diode–laser data (*17*) served as a guide for identifying and assigning the main bands of the five isotopomers, and the method of combination differences was used to confirm those assignments. Hot bands were identified and assigned by using predictions made from the molecular constants derived from the least-squared fitting of the fundamental bands and any hot bands already identified for each isotopomer.

A total of 1228 *P* and *R* lines were assigned in the first eight $\Delta v = -1$ sequence bands of the ^{74}GeO isotopomer, 1223 lines in the (1–0) to (8–7) bands of ^{72}GeO, 1029 in the (1–0) to (7–6) bands of ^{70}GeO, 789 lines in the (1–0) to (6–5) bands of ^{73}GeO, and 848 lines in the (1–0) to (7–6) bands of ^{76}GeO. Some lines were obscured by absorption due to residual impurities such as water vapor and GeH_4, and many other lines are blended; this is illustrated by the segment of the GeO spectrum shown in Fig. 3. For the unblended FTIR data used in the present analysis, the line position uncertainties were estimated to be ca. 0.002 cm^{-1}.

Data from the diode laser experiments of Thompson *et al.* (*17*) (average uncertainty 0.00055 cm^{-1}) were taken as the calibration standard. Some 90 matching transitions from the measured FTIR spectrum and the diode–laser experiment were fitted to the expression $\nu_{DL}(i) = A \times \nu_{FT}(i)$, where $\nu_{DL}(i)$ are the diode–laser data and $\nu_{FT}(i)$ the measured FTIR transition frequencies used to determine the calibration factor $A = 1.000001869$. A list of all the measured FTIR lines (after calibration) and their residuals from the combined isotopes direct potential fit analysis (see Section IV) are available from the authors or from the Journal's home page. An overview of the extent and range of the three types of data used in the present analysis is presented in Table 1.

TABLE 1
Overview of GeO ($X^1\Sigma^+$) Data Used in the Present Combined Isotopomer Analysis

		FTIR data			diode laser data			microwave data		
isotopomer	abundance	v_{max}	J_{max}	#lines	v_{max}	J_{max}	#lines	v_{max}	J_{max}	#lines
$^{70}Ge^{16}O$	21.2%	7	100	1029	5	82	19	1	0	2
$^{72}Ge^{16}O$	27.7%	8	103	1223	6	80	27	1	0	2
$^{73}Ge^{16}O$	7.7%	6	90	789	4	80	15	0	0	1
$^{74}Ge^{16}O$	35.9%	8	110	1228	6	79	25	2	0	5
$^{76}Ge^{16}O$	7.4%	7	91	848	5	78	12	1	0	2

IV. ANALYSIS

A. Combined Isotopomer Dunham-Type Analysis

In all of the fits reported herein, the observed transition energies were weighted by the inverse square of their uncertainties, and the quality of fit is indicated by the value of dimensionless standard error

$$\bar{\sigma}_f = \left\{ \frac{1}{N-M} \sum_{i=1}^{N} \left[\frac{y_{\text{calc}}(i) - y_{\text{obs}}(i)}{u(i)} \right]^2 \right\}^{1/2}, \qquad [1]$$

where each of the N experimental data $y_{\text{obs}}(i)$ has an uncertainty of $u(i)$, and $y_{\text{calc}}(i)$ is the value of datum i predicted by the M parameter model being fitted. All parameter uncertainties quoted here are 95% confidence limit uncertainties, and the atomic masses used in the combined isotope analysis were taken from the 1993 mass table (*26*).

The first stage of the analysis consisted of fitting to separate Dunham expansions for each isotopomer. In all cases, the residual discrepancies were comparable to the experimental uncertainties ($\bar{\sigma}_f < 1$), and the internal consistency of the fits showed that there were no misassignments or anomalies in these data sets. However, the total number of independent parameters required to represent the data for the five isotopomers ($5 \times 11 = 55$) was rather large.

To simplify the representation of these data sets and to search for physically interesting information about Born–Oppenheimer breakdown effects, all of the 5117 FTIR lines, the 98 diode laser measurements (*17*), and the 12 microwave data (*5*, *6*) for the five isotopomers were simultaneously fitted to a combined isotopomer Dunham-type expression for the level energies. Following Ref. (*27*), observed transitions for isotopomer α of species A–B formed from atoms of mass M_A^α and M_B^α were expressed as differences between level energies written as

$$E^\alpha(v,J) = \sum_{(l,m)\neq(0,0)} Y_{l,m}^1 \left(\frac{\mu_1}{\mu_\alpha}\right)^{m+l/2} (v+\tfrac{1}{2})^l [J(J+1)]^m + \sum_{(l,m)\geq(0,0)} \left\{ \frac{\Delta M_A^\alpha}{M_A^\alpha} \delta_{l,m}^A + \frac{\Delta M_B^\alpha}{M_B^\alpha} \delta_{l,m}^B \right\} \times \left(\frac{\mu_1}{\mu_\alpha}\right)^{m+l/2} (v+\tfrac{1}{2})^l [J(J+1)]^m, \qquad [2]$$

where $\Delta M_A^\alpha = M_A^\alpha - M_A^1$, and $\alpha = 1$ identifies a selected reference species, in this case, the most abundant isotopomer, $^{74}Ge^{16}O$. This expression is equivalent to the familiar Ross–Eng–Kildal–Bunker–Watson (*28*–*30*) expansion, except that the Born–Oppenheimer and JWKB breakdown terms are included as additive rather than multiplicative corrections and the reference species (isotopomer $\alpha = 1$, $^{74}Ge^{16}O$) is a real physical molecule. The conventional Dunham constants for other ($\alpha \neq 1$) isotopomers are generated from

$$Y_{l,m}^\alpha = \left\{ Y_{l,m}^1 + \frac{\Delta M_A^\alpha}{M_A^\alpha} \delta_{l,m}^A + \frac{\Delta M_B^\alpha}{M_B^\alpha} \delta_{l,m}^B \right\} \left(\frac{\mu_1}{\mu_\alpha}\right)^{m+l/2}. \qquad [3]$$

Other advantages of this expansion are discussed elsewhere (*27*).

The complete five-isotopomer data set was fitted to Eq. [2] using program DSParFit (*27*), which simplifies the resulting parameters by applying the sequential rounding and refitting procedure described in Ref. (*31*). This yielded the molecular constants given in the first column of Table 2. The leading vibrational Born–Oppenheimer breakdown correction coefficient seen there yields a small improvement in the quality of fit and is moderately well determined.

For the user's convenience, the Dunham parameters for the minority isotopomers generated by substituting the fitted parameters of column 1 into Eq. [3], rounded at the first digit of the parameter sensitivity (*31*), are shown in the last four columns of Table 2. More significant digits are required to represent these derived constants adequately, as the compensating changes associated with the sequential rounding and

TABLE 2
Parameters for $X^1\Sigma^+$ State GeO (all in cm^{-1}) Obtained by Fitting all FTIR, Diode Laser, and Microwave Data to Eq. [2]

constant	All-isotopomer Fit $^{74}Ge^{16}O$	Generated from the $^{74}Ge^{16}O$ constants and Eq.(3) $^{70}Ge^{16}O$	$^{72}Ge^{16}O$	$^{73}Ge^{16}O$	$^{76}Ge^{16}O$
$Y_{1,0}$	986.4928 (3)	991.49599	988.92884	987.69264	984.17822
$Y_{2,0}$	−4.47014 (15)	−4.515593	−4.492242	−4.481019	−4.44919
10^3 $Y_{3,0}$	4.65 (3)	4.7211	4.6845	4.6670	4.6173
10^3 $Y_{4,0}$	−0.010 (2)	−0.0102	−0.0101	−0.01005	−0.00991
$Y_{0,1}$	0.4856974 (2)	0.49063606	0.4880989	0.48687949	0.48342112
10^4 $Y_{1,1}$	−30.7832 (8)	−31.25390	−31.01179	−30.89565	−30.56705
10^4 $Y_{2,1}$	0.01261 (22)	0.012868	0.012735	0.012671	0.012492
10^4 $Y_{3,1}$	−0.00009 (2)	−0.0000923	−0.0000911	−0.0000905	−0.0000889
10^8 $Y_{0,2}$	−47.086 (13)	−48.048	−47.553	−47.315	−46.646
10^8 $Y_{1,2}$	−0.0617 (7)	−0.06328	−0.06247	−0.06208	−0.06098
10^{14} $Y_{0,3}$	−8. (1)	−8.2	−8.1	−8.1	−7.9
$\delta^{Ge}_{1,0}$	−0.008 (2)	–	–	–	–
No. of data	5227	1050	1252	805	862
No. parameters	12	0	0	0	0
$\overline{\sigma}_f$	0.800	0.771	0.731	0.871	1.006

Note. The numbers in parentheses are the 95% confidence limit uncertainties in the last significant digits shown.

refitting procedure do not come into play. The results in the last row of this table show that the rounded constants generated from the $^{74}Ge^{16}O$ parameters determined from the combined isotopomer analysis reproduce the input data for the individual minority isotopomers with no significant loss of precision.

B. Combined Isotopomer Direct Potential Fit Analysis

As a more compact and more physically significant alternative to the Dunham-type analysis reported above, all data for the various isotopomers of a given species were also fitted directly to eigenvalue differences numerically calculated from the effective radial Schrödinger equation

$$\left\{ -\frac{\hbar^2}{2\mu}\frac{d^2}{dR^2} + V^{\alpha}_{ad}(R) + \frac{\hbar^2 J(J+1)}{2\mu R^2} \times [1 + q^{\alpha}(R)] - E_{v,J} \right\} \psi_{v,J}(R) = 0, \quad [4]$$

where the effective adiabatic potential for isotopomer α is written as that for the most abundant isotopomer ($\alpha = 1$ again refers to $^{74}Ge^{16}O$) plus atomic mass-dependent (adiabatic) potential correction functions

$$V^{\alpha}_{ad}(R) = V^{1}_{ad}(R) + \frac{\Delta M^{\alpha}_A}{M^{\alpha}_A}\Delta V^{A}_{ad}(R) + \frac{\Delta M^{\alpha}_B}{M^{\alpha}_B}\Delta V^{B}_{ad}(R) \quad [5]$$

and the (nonadiabatic) effective centrifugal distortion correction function is

$$q^{\alpha}(R) = \frac{M^{1}_A}{M^{\alpha}_A} q_A(R) + \frac{M^{1}_B}{M^{\alpha}_B} q_B(R). \quad [6]$$

Although they depend on the choice of reference isotopomer, both the potential correction functions $\Delta V^{A,B}_{ad}(R)$ and the centrifugal correction functions $q_{A,B}(R)$ are isotopomer independent (*27*). The above description is equivalent to the Hamiltonian discussed by Watson (*32, 30*) and used in numerous practical analyses (*33–36*), except that the reference potential here is the actual effective adiabatic potential for a real isotopic molecular species (here $^{74}Ge^{16}O$), rather than the theoretical "clamped nuclei" potential obtained in the lowest order version of the Born–Oppenheimer separation (*37, 38*). Further discussion of this representation of the effective radial potential may be found in Ref. (*27*).

In the present work, the effective adiabatic potential for the dominant isotopomer was represented by the "expanded Morse oscillator" (EMO) function

$$V^{1}_{ad}(R) = D_e\{1 - e^{-\beta(z)(R-R_e)}\}^2, \quad [7]$$

where $z \equiv (R - R_e)/(R + R_e)$ and both $\beta(z)$ and the mass-dependent potential and centrifugal correction functions are simple power series in z

$$\beta(z) = \sum_{j=0} \beta_j z^j \quad [8]$$

$$\Delta V^{A}_{ad} = \sum_{j=1} u^{A}_j z^j, \quad \Delta V^{B}_{ad} = \sum_{j=1} u^{B}_j z^j \quad [9]$$

TABLE 3

Parameters of EMO Potential for Ground State GeO Obtained on Directly Fitting to All (Multiple Isotopomer) FTIR, Diode Laser, and Microwave Data

Parameter	$^{74}Ge^{16}O$
D_e / cm^{-1}	55200. (700)[a]
R_e / Å	1.6246451 (3)
β_0 / Å^{-1}	1.85418749 (38)
β_1 / Å^{-1}	−0.24733 (5)
β_2 / Å^{-1}	0.9872 (2)
β_3 / Å^{-1}	2.933 (17)
β_4 / Å^{-1}	4.2 (1)
u_1^{Ge} / cm^{-1}	−3.6 (7)
No. of data	5227
No. parameters	7
$\bar{\sigma}_f$	0.803

[a] D_e was fixed at the thermochemically determined value (*37*).

$$q_A(R) = \sum_{j=0} q_j^A z^j, \quad q_B(R) = \sum_{j=0} q_j^B z^j. \qquad [10]$$

In these expansions, the units of all $\{\beta_j\}$ coefficients are Å^{-1}, those of the $\{u_j^A\}$ and $\{u_j^B\}$ coefficients are cm^{-1}, and the $\{q_j^A\}$ and $\{q_j^B\}$ expansion coefficients are all dimensionless.

The numerical integration of Eq. [4] was performed on the interval 0.2 Å $\geq r \geq$ 13.0 Å with a grid spacing of 0.0004 Å. This sufficed to ensure that the eigenvalues used in the fits were converged to better than 0.000001 cm^{-1} for levels observed with the microwave data ($v = 0$ and 1) and to better than 0.0001 cm^{-1} for levels seen in the infrared ($v \leq 8$).

The highest observed levels included in the present analysis lie approximately 7600 cm^{-1} above the potential minimum. As this is less than $\frac{1}{7}$ of the reported ground state dissociation energy, in the present analysis D_e was fixed at the literature value of 55 200 (±700) cm^{-1} (*39*).

As in the Dunham-type parameter fits of Section IV.A, it was found that inclusion of Born–Oppenheimer breakdown $\Delta V_{ad}^{A,B}$ or $q^{\alpha}(R)$ functions had only a modest effect on the value of $\bar{\sigma}_f$, and only the leading term in the Ge–atom potential correction function could be determined with any significance. However, as with the present Dunham-type analysis, this is one of the first heavy metal systems for which such atomic mass-dependent correction terms have been determined.

The results of this direct potential fit analysis are summarized in Table 3. As is seen there, the quality of fit is essentially identical to that obtained from the parameter-fit analysis of Eq. [2] and Table 2, except that the potential-fit analysis requires significantly fewer parameters (7 instead of 12). Again, the parameters are rounded without loss of precision using the sequential rounding and refitting procedure of Ref. (*31*).

While the quality of fit is essentially the same in the Dunham and direct potential fit analyses, the latter is to be preferred for two reasons. The first is that the resulting potential energy function is quantum mechanically accurate, while a potential function determined by the RKR method from the Dunham constants of Table 2 would only be as accurate as the first-order JWKB approximation. The second is that this quantum mechanical potential should yield reliable predictions for very large J (*40*), while long J extrapolations with empirical molecular constants such as those in Table 2 are notoriously unreliable.

ACKNOWLEDGMENTS

We thank Professor A. Anderson for his help with helium transfers. This research was supported by the Natural Sciences and Engineering Research Council of Canada and in part by the Petroleum Research Fund of the American Chemical Society.

REFERENCES

1. V. Kellö and A. J. Sadlej, *J. Chem. Phys.* **98,** 1345–1351 (1993).
2. J. Leszczyński and J. S. Kwiatkowski, *J. Phys. Chem.* **97,** 12189–12192 (1993).
3. Z. Barandiarán and L. Seijo, *J. Chem. Phys.* **101,** 4049–4054 (1994).
4. F. L. Sefyani, J. Schamps, and D. Duflot, *J. Quant. Spectrosc. Radiat. Transfer* **54,** 1027–1034 (1995).
5. T. Törring, *Z. Naturforsch. A* **21,** 287–289 (1966).
6. R. Honerjäger and R. Tischer, *Z. Naturforsch. A* **28,** 1374–1375 (1973).
7. G. Hager, L. E. Wilson, and S. G. Hadley, *Chem. Phys. Lett.* **27,** 439–441 (1974).
8. G. Hager, R. Harris, and S. G. Hadley, *J. Chem. Phys.* **63,** 2810–2820 (1975).
9. G. A. Capelle and J. M. Brom, *J. Chem. Phys.* **63,** 5168–5176 (1975).
10. E. A. Colbourn, J. M. Dyke, A. Fackerell, A. Morris, and I. R. Trickle, *J. Chem. Soc., Faraday Trans. II* **74,** 2278–2285 (1978).
11. A. Lagerqvist and I. Renhorn, *Phys. Scr.* **25,** 241–256 (1982).
12. O. Appelbald, S. Fredlin, and A. Lagerqvist, *Phys. Scr.* **25,** 933–938 (1982).
13. O. Appelblad, S. Fredlin, A. Lagerqvist, and F. Alberti, *Phys. Scr.* **28,** 160–170 (1982).
14. W. Żyrnicki, *J. Mol. Spectrosc.* **89,** 557–560 (1981).
15. J. S. Odgen and M. J. Ricks, *J. Chem. Phys.* **52,** 352–357 (1970).
16. A. Bos, *J. Phys. Chem.* **78,** 1763–1769 (1974).
17. G. A. Thompson, A. G. Maki, and A. Weber, *J. Mol. Spectrosc.* **116,** 136–142 (1986).
18. K. P. Huber and G. Herzberg, "Constants of Diatomic Molecules," Van Nostrand, Toronto, 1979.
19. F. Vega, C. N. Afonso, and J. Solis, *App. Surf. Sci.* **69,** 403–406 (1993).
20. K. Prabhakaran, T. Nishioka, K. Sumitomo, Y. Kobayashi, and T. Ogino, *Appl. Phys. Lett.* **62,** 864–866 (1993).
21. P. F. Bernath, *Chem. Soc. Rev.* **25,** 111–115 (1996).
22. I. Mills, T. Cvitaš, K. Homann, N. Kallay, and K. Kuchitsu, "Quantities, Units and Symbols in Physical Chemistry," 2nd ed., Blackwell Sci., Oxford, 1993.
23. J. Brault, program PC/DECOMP, version 2.60, 1993.
24. P. F. Bernath, "Spectra of Atoms and Molecules," Oxford Univ. Press, Oxford, 1995.
25. C. N. Jarman, program Loomis–Wood, version 2.0, 1993.

26. G. Audi and A. H. Wapstra, *Nucl. Phys.* 1–65 (1993).
27. R. J. Le Roy, *J. Mol. Spectrosc.* **194,** 189 (1999).
28. A. H. M. Ross, R. S. Eng, and H. Kildal, *Opt. Commun.* **12,** 433–438 (1974).
29. P. R. Bunker, *J. Mol. Spectrosc.* **68,** 367–371 (1977).
30. J. K. G. Watson, *J. Mol. Spectrosc.* **80,** 411–421 (1980).
31. R. J. Le Roy, *J. Mol. Spectrosc.* **191,** 223–231 (1998).
32. J. K. G. Watson, *J. Mol. Spectrosc.* **45,** 99–113 (1973).
33. J. A. Coxon and P. G. Hajigeorgiou, *J. Mol. Spectrosc.* **150,** 1–27 (1991).
34. H. G. Hedderich, M. Dulick, and P. F. Bernath, *J. Chem. Phys.* **99,** 8363–8370 (1993).
35. M. Dulick, K.-Q. Zhang, B. Guo, and P. F. Bernath, **188,** 14–26 (1998).
36. J. A. Coxon and P. G. Hajigeorgiou, *J. Mol. Spectrosc.* **193,** 306–318 (1999).
37. M. Born and J. R. Oppenheimer, *Ann. Phys.* **84,** 457–484 (1927).
38. W. Kołos and L. Wolniewicz, *J. Chem. Phys.* **41,** 3663–3673 (1964).
39. J. Drowart, F. Degrève, G. Verhagen, and R. Colin, *Trans. Faraday Soc.* **61,** 1072–1085 (1965).
40. J. Y. Seto and R. J. Le Roy, unpublished manuscript, 1998.